

“Pudding mold” band drives large thermopower in Na_xCoO_2

Kazuhiko Kuroki¹ and Ryotaro Arita²

¹ *Department of Applied Physics and Chemistry,
The University of Electro-Communications, Chofu, Tokyo 182-8585, Japan*

² *RIKEN, 2-1 Hirosawa, Wako, Saitama 351-0198, Japan*

(Dated: October 31, 2018)

In the present study, we pin down the origin of the coexistence of the large thermopower and the large conductivity in Na_xCoO_2 . It is revealed that not just the density of states (DOS), the effective mass, nor the band width, but the peculiar *shape* of the a_{1g} band referred to as the “pudding mold” type, which consists of a dispersive portion and a somewhat flat portion, is playing an important role in this phenomenon. The present study provides a new guiding principle for designing good thermoelectric materials.

For the past decade, a cobaltate Na_xCoO_2 has been one of the most highlighted materials in the field of condensed matter physics in that it exhibits large thermopower[1] and magnetism[2] in the non-hydrated sodium rich systems, and superconductivity in the hydrated sodium poor ones.[3] In particular, the discovery of large thermopower in Na_xCoO_2 [1] and the findings in cobaltates/cobaltites[4, 5, 6, 7, 8] and rhodates[9, 10] that followed have brought up an interesting possibility of finding good thermoelectric materials that have relatively large conductivity.

Theoretically, it has been proposed that the three fold degeneracy of the t_{2g} orbitals as well as the strong electron correlation effects plays an important role in these transition metal oxides.[11] Importance of spin degeneracy has been pointed out from experiments under magnetic field.[12] As for the orbital degeneracy, the t_{2g} orbitals are split into an a_{1g} orbital and two e'_g orbitals due to the crystal field, and early first principles calculation predicted six hole pockets from the e'_g bands in addition to the a_{1g} Fermi surface.[13] However, angle resolved photoemission spectroscopy (ARPES) studies [15, 16, 17, 18] have revealed that the e'_g bands lie $O(100)\text{meV} \simeq O(1000)\text{K}$ below the Fermi level. Therefore, it seems unlikely that multiorbital effects affect the thermopower at least for $T \sim O(100)\text{K}$, where a large thermopower of $S \sim O(100)\mu\text{V}/\text{K}$ is already observed.[8] On the other hand, conventional calculations of the thermopower using the LDA bands already give large values,[13, 14] suggesting that the band structure, not the electron correlation, is the key. In fact, it has been pointed out in some studies that the narrowness of the t_{2g} bands is essential. [13, 14, 19] Although the narrowness of the bands must indeed be a factor, this *alone* cannot be the origin of the large thermopower because otherwise we would expect more good thermoelectric materials. Also, the problem of how the large thermopower and the large conductivity can coexist has not been addressed clearly so far.

In the present study, we generally propose that a peculiar *shape* of the band (Fig.1(a)), like the a_{1g} band of the cobaltates (Fig.1(c)), can give large thermopower

and large conductivity at the same time. In fact, in the preceding studies, we have proposed that the superconductivity and the magnetism in Na_xCoO_2 both originate from the peculiar shape of the a_{1g} band,[20, 21] so adding the present study reveals that all of these interesting phenomena share the same origin.

Our idea is the following. Using the Boltzmann’s equation approach, the thermopower is given as[22]

$$\mathbf{S} = \frac{1}{eT} \mathbf{K}_0^{-1} \mathbf{K}_1 \quad (1)$$

where $e (< 0)$ is the electron charge, T is the temperature, tensors \mathbf{K}_0 and \mathbf{K}_1 are given by

$$\mathbf{K}_n = \sum_{\mathbf{k}} \tau(\mathbf{k}) \mathbf{v}(\mathbf{k}) \mathbf{v}(\mathbf{k}) \left[-\frac{\partial f(\varepsilon)}{\partial \varepsilon}(\mathbf{k}) \right] (\varepsilon(\mathbf{k}) - \mu)^n. \quad (2)$$

Here, $\varepsilon(\mathbf{k})$ is the band dispersion, $\mathbf{v}(\mathbf{k}) = \nabla_{\mathbf{k}} \varepsilon(\mathbf{k})$ is the group velocity, $\tau(\mathbf{k})$ is the quasiparticle lifetime, $f(\varepsilon)$ is the Fermi distribution function, and μ is the chemical potential. Hereafter, we simply refer to $(\mathbf{K}_n)_{xx}$ as K_n , and $S_{xx} = (1/eT)(K_1/K_0)$ (for diagonal \mathbf{K}_0) as S . Using K_0 , conductivity can be given as $\sigma_{xx} = e^2 K_0 \equiv \sigma = 1/\rho$. Roughly speaking for a constant τ ,

$$K_0 \sim \Sigma'(v_A^2 + v_B^2), \quad K_1 \sim (k_B T) \Sigma'(v_B^2 - v_A^2) \quad (3)$$

(apart from a constant factor) stand, where Σ' is a summation over the states in the range of $|\varepsilon(\mathbf{k}) - \mu| < \sim k_B T$, and v_A and v_B are typical velocities for the states above and below μ , respectively. In usual metals, where $v_A \sim v_B$, the positive and the negative contributions in K_1 nearly cancel out to result in a small S (Fig.1(b)). Now, let us consider a band that has a somewhat flat portion at the top (or the bottom), which sharply bends into a highly dispersive portion below (above). We will refer to this band structure as the “pudding mold” type (Fig.1(a)). For this type of band with μ sitting near the bending point, $v_A^2 \gg v_B^2$ holds for high enough temperature, so that the cancellation in K_1 is less effective, resulting in $|K_1| \sim (k_B T) \Sigma' v_A^2$ and $K_0 \sim \Sigma' v_A^2$, and thus large $|S| \sim O(k_B/|e|) \sim O(100)\mu\text{V}/\text{K}$. A similar situation where a large S originates from $v_A^2 \gg v_B^2$ can be

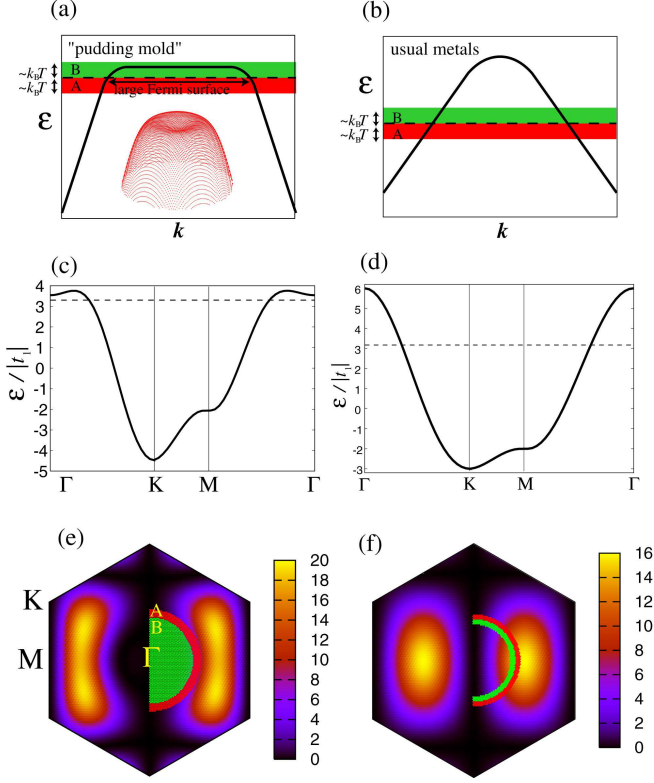


FIG. 1: (color online) Schematic figure for (a) the pudding mold band and (b) a usual metal. The inset of (a) shows the top of the band shown in (c). The band dispersion for (c) $t_2/t_1 = -0.3$, $t_3/t_1 = -0.11$ and (d) $t_2 = t_3 = 0$. The dashed line shows the position of μ at $x = 0.7$ ($n = 1.7$) and $T = 300\text{K}$. A contour plot of $[v_x(\mathbf{k})]^2$ for $x = 0.7$ and $T = 300\text{K}$ with (e) $t_2/t_1 = -0.3$, $t_3/t_1 = -0.11$ and (f) $t_2 = t_3 = 0$. Also region A (red outer half ring) and region B (green inner half circle or ring) are superposed. Only the $k_x \geq 0$ part of regions A and B is shown for clarity.

realized for a simple parabolic band if μ lies very close to the band edge, but in that case, although the relative ratio $|K_1/K_0|$ is large, K_0 is small because v_A , v_B and the Fermi surface are small, so that the conductivity is small. By contrast, for the pudding mold band, the large v_A and the large Fermi surface (in 2D and 3D) result not only in large $|K_1/K_0| \propto S$ but also in large $K_0 \propto \sigma$ as well, being able to give a large power factor S^2/ρ , which is important for device applications.[23]

We now apply the idea to Na_xCoO_2 . We take a 2D single band tight binding model $H = -\sum_{ij} t_{ij}(c_i^\dagger c_j + c_j^\dagger c_i)$ that considers hopping integrals between first, second and third nearest neighbor sites, t_1 , t_2 , and t_3 . $t_2/t_1 = -0.3$, $t_3/t_1 = -0.11$ are introduced so as to reproduce the shape of the a_{1g} portion of the bands in the first principles calculation.[13, 24] We take $t_1 = -1000\text{K}$ to reproduce the band width obtained in the ARPES data,[16, 17] which about 60% of the LDA result[13, 24] due to electron correlation. The band filling n is defined

as $n = \text{number of electrons/sites}$, and it is related to the sodium content x as $n - 1 = x$ (as far as the e'_g bands are fully filled). In Fig.1(c), we show the band dispersion, whose top around the Γ point (inset of Fig.1(a)) indeed has a form of a pudding mold.

In the calculation of S , we first neglect the \mathbf{k} dependence of τ (so that τ cancels out in K_1/K_0). In Fig.2(a), we show the temperature dependence of S for various values of band fillings. If we first focus on $x = 0.7$, we find that the overall temperature dependence observed experimentally for $x \simeq 0.71$ in ref.8 as well as its large value of $\simeq 100\mu\text{V/K}$ at $T \simeq 300\text{K}$ is reproduced. In Fig.2(c), we show the Na content dependence of S at $T = 300\text{K}$, together with the experimental data of S at 300K taken from ref.8. Here again, we find a good agreement between the calculation and the experimental results. For comparison, we show in Figs.2(b) and (c) the calculation result for $t_2 = t_3 = 0$, where the band top is just parabolic (Fig.1(d)). We see that the thermopower is strongly suppressed compared to the case with the pudding mold band. Note that for $t_2 = t_3 = 0$, the band width itself is nearly the same with the case of $t_2/t_1 = -0.30$ and $t_3/t_1 = -0.11$, which indicates that the *shape* of the band is important.

In order to see that our idea is working, we show in the bottom of Fig.1 $[v_x(\mathbf{k})]^2$, along with the regions

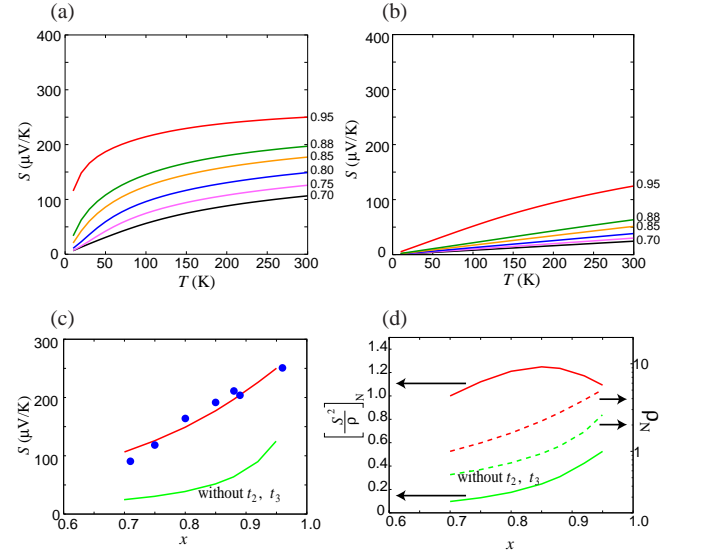


FIG. 2: (color online) (a) Thermopower for $t_2/t_1 = -0.3$ and $t_3/t_1 = -0.11$ plotted as functions of temperature for various x (denoted at the right edge). \mathbf{k} dependence of τ is not considered here. (b) Similar to (a) except $t_2 = t_3 = 0$. (c) Thermopower and (d) the normalized (normalized by the values for $x = 0.7$, $t_2/t_1 = -0.3$ and $t_3/t_1 = -0.11$) resistivity (dashed) and power factor (solid) at $T = 300\text{K}$ plotted as functions of x for $t_2/t_1 = -0.3$ and $t_3/t_1 = -0.11$ (red) and $t_2 = t_3 = 0$ (green). In (c), the experimental data at 300K (blue dots) are taken from ref.[8].

$-2k_B T < \varepsilon(\mathbf{k}) - \mu < 0$ (region A) and $0 < \varepsilon(\mathbf{k}) - \mu < 2k_B T$ (region B). It can be seen that for the pudding mold band in (e), $[v_x(\mathbf{k})]_B^2/[v_x(\mathbf{k})]_A^2 \ll 1$, while for a parabolic band in (f) ($t_2 = t_3 = 0$), $[v_x(\mathbf{k})]_B^2/[v_x(\mathbf{k})]_A^2 \simeq 1$. It is not appropriate to say that the large S is due to the large DOS that originates from the flatness of the band top, because it is the *dispersive portion* (region A) that is positively contributing to S .

The important expectation for the pudding mold band is not just the large thermopower, but also a relatively large conductivity and thus a large power factor. In Fig.2(d), we show the normalized resistivity ρ_N and the power factor $[S^2/\rho]_N$ with and without t_2 and t_3 (here the x dependence of τ is neglected). The resistivity of the pudding mold band is only about a factor of ~ 2 larger than that for $t_2 = t_3 = 0$, and this combined with the large thermopower results in a strong enhancement (10 times larger at $x = 0.7$) of the power factor.[25]

So far, we have not focused on the effect of multiple Fermi surfaces (Fig.3(a)), which has been proposed to be the origin of the superconductivity[20, 26] and the magnetism[21, 27, 28]. To see this effect, we plot in Fig.3(c) the t_3 dependence of S and $[S^2/\rho]_N$. Increasing t_3 (or t_2) makes the local minimum structure at the Γ point deeper as shown in Fig.3(b). S takes its maximum at a certain t_3 , but the power factor continues to grow. This is because there are inner and outer Fermi surfaces both contributing to the conductivity, whose increase overcomes the decrease of S . If we go back to Fig.2(d), this multiple Fermi surface effect is contributing to the low resistivity and high power factor for $x \sim 0.8$.

In this context, it is interesting to estimate how large a power factor the multiple e'_g hole pockets would give if they were present. In fact, the top of the e'_g bands around the K point is again of the pudding mold type, with some corrugation that results in the multiple pockets. If we use the effective single band dispersion that resembles the upper portion of the e'_g bands[29], we find that the power factor is about two times larger than in the a_{1g}

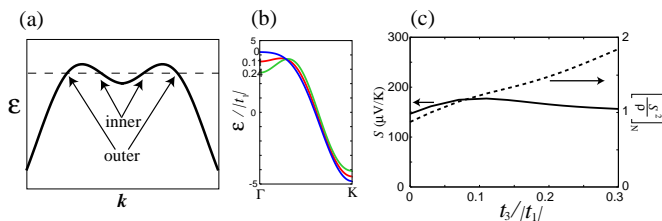


FIG. 3: (color online) (a) Schematic plot of the pudding mold band with corrugation. μ sitting at the dashed line results in inner and outer Fermi surfaces. (b) The variation of the band upon increasing $t_3/|t_1|$ as $0 \rightarrow 0.11 \rightarrow 0.24$ with $t_2/t_1 = -0.3$. (c) Thermopower (solid) and normalized power factor (dashed) plotted as functions of $t_3/|t_1|$ for $t_2/t_1 = -0.3$, $x = 0.85$ and $T = 300\text{K}$.

case shown in Fig.2(d). Thus, if it were possible to push up the e'_g bands so that the band top comes above the Fermi level for high Na content, the combined effect of both a_{1g} and e'_g pudding mold bands may result in a very large power factor. Apart from this possibility, at high temperatures, and for relatively small Na content, where the Fermi level should sit close to the e'_g band top, holes may be introduced at the top of the e'_g band, which may be related to the enhancement of the thermopower above 500K observed in ref.[5]

We have seen that the consideration of the peculiar shape of the a_{1g} band alone suffices to understand the experimentally observed thermopower for $x \simeq 0.7$ or $T \simeq 300\text{K}$. For $x \geq 0.8$ and $T < 200\text{K}$, however, this is not the whole story. In the calculated thermopower in Fig.2(a), a hump structure around 100K found in the experiment for $x \geq 0.8$ [8] is not reproduced. In fact, this Na content and the temperature range is close to the region where the metallic magnetism, or the spin density wave (SDW), [2] sets in (Fig.4(a)), whose origin has been shown to be due to the nesting between the inner and the outer portions of the Fermi surface. [21, 27] When the system is close to the SDW instability, the spin fluctuations become localized in \mathbf{q} space around the nesting vector \mathbf{Q} and in energy around $\omega \sim 0$. Thus, the quasiparticle scatterings by spin fluctuations occur with momentum transfer close to \mathbf{Q} and with small energy transfer, so that, assuming a nearly isotropic Fermi surface, only the quasiparticles with $|\varepsilon(\mathbf{k}) - \mu| < E_B(T)$ is strongly scattered, where $E_B(T)$ is a certain energy scale that decreases with temperature (Fig.4(b)). We leave microscopic treatment of this effect for future study,[30] but here, in order to qualitatively take this effect into account, we assume a trial form of τ as $1/\tau(\mathbf{k}, T) \propto A^2(\mathbf{k}, T)T + [1 - A^2(\mathbf{k}, T)]T^2/\xi_1$, $A(\mathbf{k}, T) = \cosh^{-1}\{[\varepsilon(\mathbf{k}) - \mu(T)]/E_B(T)\}$. This form assumes that τ in the strongly scattered regime is proportional to $1/T$, while it crosses over to $1/T^2$ in the weakly scattered regime. For $E_B(T)$, we assume a form $E_B(T) = k_B T (T/\xi_2)^\gamma + \Delta_0(x)$, where ξ_2 is the temperature scale below which $E_B(T)$, apart from Δ_0 , becomes smaller than the energy scale ($\sim k_B T$) relevant for K_0 and K_1 . We vary Δ_0 with x as shown in Fig.4(c) so as to reflect the tendency towards the SDW formation, which is the strongest around $x = 0.8 \sim 0.85$ experimentally. S , the Peltier conductivity $\alpha = S\sigma$, and ρ (Fig.4(d)-(f)) calculated by using this τ and taking $\gamma = 2$, $\xi_1 = 1$, and $\xi_2 = 0.1$ (in units of $|t_1|$) indeed reproduce the experimental results at least qualitatively. At low temperatures for $x \geq 0.75$, α exhibits a maximum and ρ crosses over from T to T^2 dependence in rough agreement with the experiment.[8] This is because the quasiparticles somewhat away from the Fermi surface have enhanced lifetime at low temperatures.[31] The thermopower $S = \alpha/\sigma$ now has the hump structure at low temperatures for $x \geq 0.8$ because $K_1 \propto \alpha T$ is enhanced more than $K_0 \propto \sigma$ since the former has larger contribution from the states away

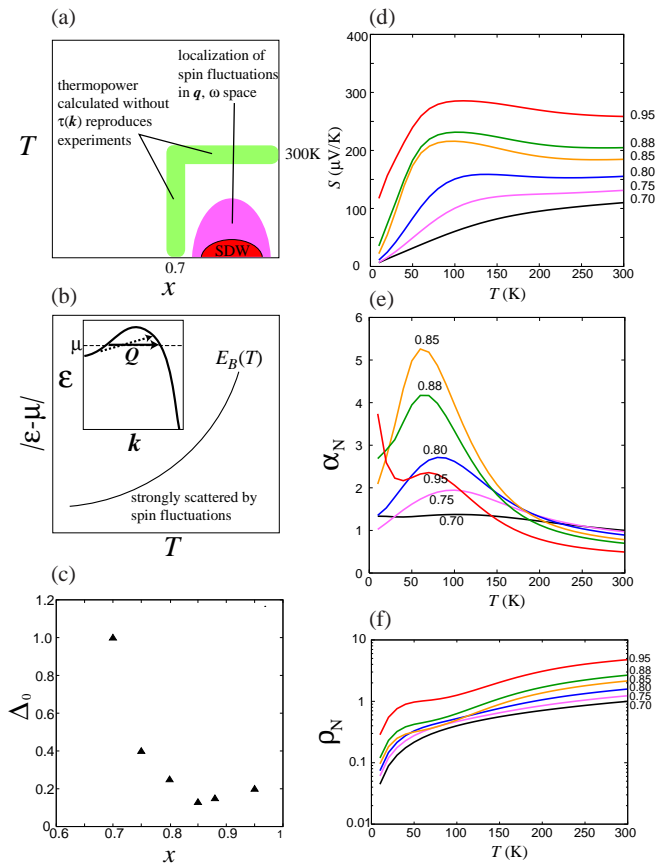


FIG. 4: (color online) (a) Schematic phase diagram concerning the relation between SDW and the thermopower. (b) The inset shows that when the spin fluctuations are localized in \mathbf{q}, ω space, the quasiparticle scatterings by spin fluctuations occur mainly with momentum transfer close to the nesting vector \mathbf{Q} and with low energy transfer (solid arrow), while scattering with other \mathbf{q} and large ω (dashed arrow) is less effective. Shown in the main panel is a schematic plot of the energy scale $E_B(T)$ under which strong scatterings take place. (c) Variation of Δ_0 with x . Calculation result for (d) the thermopower S , (e) the normalized Peltier conductivity α_N and (f) the normalized resistivity ρ_N (normalized by the values at $x = 0.7$ and $T = 300\text{K}$) for various x using the trial form for τ with $\gamma = 2$, $\xi_1 = 1$ and $\xi_2 = 0.1$ (in units of $|t_1|$).

from the Fermi surface due to the factor $(\varepsilon(\mathbf{k}) - \mu)$ in eq.(2). At present, our form of τ has no microscopic basis, so we do not persist in these particular parameter values. In fact, for $x = 0.85$, e.g., by taking $\gamma = 1$, $\xi_2 = 0.06$, $\Delta_0 = 0.08$, a similar curve for S but with a smaller hump is obtained.

To summarize, we have pinned down the origin of the coexistence of the large thermopower and the large conductivity in Na_xCoO_2 : the pudding mold a_{1g} band that has a dispersive portion and a flat portion with some corrugations at the top that can result in multiple Fermi surfaces. The present study provides a new guiding principle for designing good thermoelectric materials: look for ma-

terials that have pudding mold band(s) with the chemical potential lying close to its bending point. Roughly speaking, pudding mold bands tend to occur in geometrically frustrated lattice structures because there are several hopping contributions to $\varepsilon(\mathbf{k})$, which nearly cancel at some \mathbf{k} , while not at other \mathbf{k} . This, however, does not mean that “seemingly nonfrustrated” lattices are always not good since, for example, a square lattice with sufficiently large diagonal hopping integrals (t') in addition to vertical and horizontal hoppings (t) also results in a pudding mold band and a large thermopower (e.g., for $t = -1$ and $t' = 0.45$, $S \simeq 200\mu\text{V/K}$ at $T = 0.3|t|$ and $n = 1.80$). Another caution is that, even if a pudding mold band is present, a coexistence of a dispersive metallic band with a much larger K_0 and a small K_1 would result in a suppression of $(\sum_{\text{bands}} K_1^{\text{band}})/(\sum_{\text{bands}} K_0^{\text{band}})$ and thus a small total thermopower. Therefore, reliable band structure calculation is necessary in order to design good thermoelectric materials based on the present guiding principle.

Numerical calculations were performed at the facilities of the Supercomputer Center, ISSP, University of Tokyo. This study has been supported by Grants-in-Aid for Scientific Research from the Ministry of Education, Culture, Sports, Science and Technology of Japan, and from the Japan Society for the Promotion of Science.

-
- [1] I. Terasaki *et al.*, Phys. Rev. B **56**, R12685 (1997).
 - [2] T. Motohashi *et al.*, Phys. Rev. B **67**, 064406 (2003).
 - [3] K. Takada *et al.*, Nature **422**, 53 (2003).
 - [4] S. Li *et al.*, J. Mater. Chem. **9**, 1659 (1999).
 - [5] K. Fujita *et al.*, Jpn. J. Appl. Phys. **40**, 4644 (2001).
 - [6] S. Hébert *et al.*, Phys. Rev. B **64**, 172101 (2001).
 - [7] Y. Miyazaki *et al.*, J. Phys. Soc. Jpn. **71**, 491 (2002).
 - [8] M. Lee *et al.*, Nature Materials **5**, 537 (2006).
 - [9] S. Okada and I. Terasaki, Jpn. J. Appl. Phys. **44**, 1834 (2005).
 - [10] Y. Okamoto *et al.*, J. Phys. Soc. Jpn. **75**, 023704 (2006).
 - [11] W. Koshibae and S. Maekawa, Phys. Rev. Lett. **87**, 236603 (2001).
 - [12] Y. Wang *et al.*, Nature **423**, 425 (2003).
 - [13] D.J. Singh, Phys. Rev. B **61**, 13397 (2000).
 - [14] G.B. Wilson-Short *et al.*, Phys. Rev. B **75** 035121 (2007).
 - [15] M.Z. Hasan *et al.*, Phys. Rev. Lett. **92**, 246402 (2004).
 - [16] H.-B. Yang *et al.*, Phys. Rev. Lett. **92**, 246403 (2004); *ibid.* **95**, 146401 (2005).
 - [17] T. Takeuchi *et al.*, Proc. 24th Int. Conf. Thermoelectrics (IEEE, Piscataway, NJ, 2005) 435.
 - [18] T. Shimojima *et al.*, Phys. Rev. Lett. **97**, 267003 (2006).
 - [19] T. Takeuchi *et al.*, Phys. Rev. B **69**, 125410 (2004).
 - [20] K. Kuroki *et al.*, Phys. Rev. B **73**, 184503 (2006).
 - [21] K. Kuroki *et al.*, Phys. Rev. Lett. **98**, 13601 (2007).
 - [22] e.g., N.W. Ashcroft and N.D. Mermin, *Solid State Physics* Thomson Learning (1976).
 - [23] e.g., G.D. Mahan, *Solid State Physics* **51**, 81 (1997).
 - [24] K.-W. Lee *et al.*, Phys. Rev. B **70**, 045104 (2004)
 - [25] The origin of the strong enhancement of the power fac-

tor differs from the common knowledge that a parabolic band with large effective mass m^* gives a large thermopower. For a fixed carrier density, the thermopower for the parabolic band is proportional to m^* , [22] but this can be attributed solely to $K_0 \propto \sigma \propto 1/m^*$, while K_1 is independent of m^* . Thus, the power factor $\propto K_1^2/K_0$ is only proportional to the resistivity. By contrast, in the pudding mold case, the flat portion of the band contributes to an increase of K_1 , so that an increase of only a factor of 2 in the resistivity can result in a power factor 10 times larger.

[26] M. Mochizuki and M. Ogata, J. Phys. Soc. Jpn. **75**,

113703 (2006); *ibid* **76**, 013704 (2007); M. Mochizuki *et al.*, J. Phys. Soc. Jpn. **76**, 023702 (2007).

[27] M.M. Korshunov *et al.*, JETP Lett. **84**, 650 (2007); Phys. Rev. B **75**, 094511 (2007).

[28] D. Yoshizumi *et al.*, cond-mat/0704.1065.

[29] K. Kuroki *et al.* Phys. Rev. Lett. **93**, 077001 (2004).

[30] A microscopic investigation on this issue may require a 3D model, since the actual Fermi surface nesting is 3D.[21]

[31] The deviation of ρ and α from the experiments below 50K is due to the divergence of $\tau(\mathbf{k})$ at very low temperatures, which should not occur in actual materials.